

Noise Studies for the San Antonio "Y" Project

GRANT S. ANDERSON

ABSTRACT

Measurements were made in Austin, Texas, of highway traffic noise reflecting from the underside of an overhead roadway to diagnose these reflections and the resulting amplification to the side. Special care was taken to normalize all measurements to the actual emission level of each passing truck. It was determined that reflections from the precast I girders were scattered to the side rather than reflected specularly. An equation was developed that related this scattered sound to the relevant cross-sectional geometry at the two measurement sites. Subsequent measurements at two additional sites verified the scattering equations to within 1 dB, on average. For different cross-sectional geometries in San Antonio, where the proposed structure is a composite wing girder rather than a precast I girder, calculations were made of the sideline amplification caused by the expected specular reflections. Comparison of these calculated (specular) results with the measured (scattered) results in Austin indicates that the San Antonio amplification should be less than that measured in Austin, except when both of the following occur: (a) the receiver is within 50 to 60 ft of the edge of the elevated structure, and (b) the upper roadway curves away from the receiver.

Figure 1 shows a portion of I-35 in Austin, Texas, where the Interstate is split level: half the traffic is depressed and the other half is elevated. Along this portion of I-35 the Texas State Department of Highways and Public Transportation (TSDHPT) had received complaints that the elevated structure was amplifying traffic noise to the side by reflecting sound from its underside. Attempts to measure this possible amplification had been inconclusive.

Of immediate concern was a similar split-level Interstate proposed for San Antonio. Would the proposed San Antonio structure amplify noise levels above what was predicted from the standard FHWA equations? If so, by how much?

Figure 2 shows the two elevated structures for Austin and San Antonio. The Austin structure consists of a precast concrete deck supported on steel I girders. When sound reflects from the underside of such a structure, a portion of it is reflected specularly as from a mirror, where the angle of reflection equals the angle of incidence.

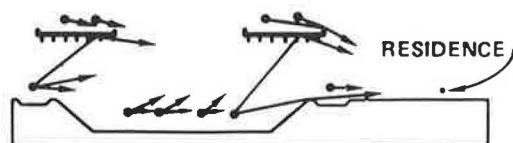
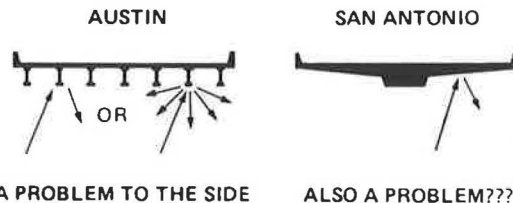


FIGURE 1 Complete measurement geometry in Austin.



A PROBLEM TO THE SIDE ALSO A PROBLEM???

FIGURE 2 The two elevated structures.

Another portion is scattered in all directions on reflection. For the Austin structure, the relative strengths of these reflected components are not obvious.

By comparison, reflection from the San Antonio structure is surely specular. This proposed structure--a so-called composite wing girder--consists of broad expanses of flat concrete devoid of any exposed beams. Because the two structures are so different from an acoustical point of view, amplification to the side in Austin does not necessarily mean similar amplification in San Antonio.

A three-part investigation of this type of amplification is discussed in this paper:

1. Measurement of the amplification in Austin,
2. Diagnosis of the reflected sound in Austin to determine if it is predominantly specular or predominantly scattered, and
3. Application of the Austin results to predict possible amplification in San Antonio.

The results are summarized as follows. Austin amplification was measured to range between zero and 12 dB, depending on receptor distance to the side. The diagnosis clearly indicates that Austin reflections are predominantly scattered. As a result, the Austin measurements are no help in predicting possible amplification in the San Antonio structure.

The amplification of the San Antonio structure was computed by assuming specular reflections from the underside of the elevated structure. The resulting amplifications range between zero and 7 dB, but most are usually between zero and 3 dB.

The remainder of this paper contains details of the Austin measurements and their mathematical analysis, followed by details of the resulting amplifications and diagnosis of the reflected sound. Additional Austin verification measurements are also given. Finally, the predictions of amplification in San Antonio are described.

AUSTIN MEASUREMENTS: AN OVERVIEW

Figure 1 shows the Austin cross-sectional geometry. Two sites were chosen for measurement: one depressed 18 ft and the other depressed 12 ft. The geometrical complexity is obvious from the figure. With this geometry, the component of the sound reflected from the structure may not predominate enough to be measured at all by using the time-averaging descriptor L_{eq} .

To eliminate this complication during diagnosis, peak passby levels were measured for individual heavy trucks on the lower roadway, rather than the

L_{eq} . As long as no other trucks are close by during each peak measurement, the uncontaminated measurement shown in Figure 3 results. In Figure 3 the total level at the microphone consists of two components: a direct component and a reflected component.

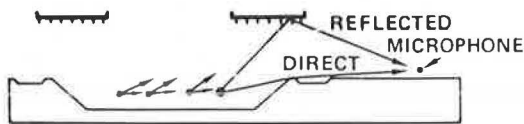
Depressed sections were chosen for measurement so that the reflected component would dominate over the direct component, which is reduced by diffraction over the top edge of the retaining wall. Even though this reflected component dominates, the direct component must still be subtracted from the total at the receptor to precisely determine the reflected component. The only recourse is to compute this direct component.

Errors inherent in this computation will not significantly affect the result of the subtraction as long as the reflected component dominates. The introduction of a computation into the analysis adds another complication, however. Computation of the direct component for an individual truck passby includes an emission-level term. Rather than assume that the noise emission from each vehicle is equal to the national average, precision is maintained by an independent measurement of the emission level of each vehicle as it passes. Measurement of emission level is not straightforward, however, because an uncontaminated measurement 50 ft to the side is impossible. Instead, a surrogate is used for emission level, which is measured at a reference microphone directly above the median and high enough so that essentially no reflected sound reaches it. The resulting geometry is shown in Figure 4. The peak reference level as a truck passes by is a measure of the noise emissions from that vehicle, but upwards at an angle rather than to the side, and not at the standard distance.

In summary, the diagnosis uses measurements of single truck passbys, simultaneously measured to the side and at the reference position. The reference level is used to normalize the entire analysis to the emission level of that particular truck. The (computed) direct component is subtracted from the total level L_T at the microphone to yield the reflected component L_R . It is this reflected component that is then quantified and diagnosed as specular, scattered, or a mixture of the two.

ANALYSIS OF AUSTIN MEASUREMENTS

Two equations are basic to the analysis. The first relates the amplification of the structure to the measured L_{Total} and the computed L_{Direct} :



$$\text{AMPLIFICATION} = \text{TOTAL} - \text{DIRECT}$$

FIGURE 3 Measurement geometry for one lane and receptor pair.

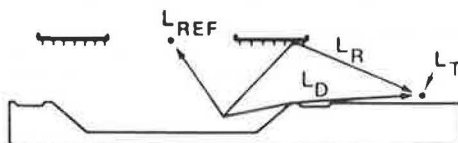


FIGURE 4 Measurement geometry with reference microphone.

$$\text{Amplification} = L_{Total} - L_{Direct} \quad (1)$$

For example, if the direct component is 67 dB(A), this would also be the sound level at the receptor in the absence of the elevated structure. If the measured L_{Total} is 75 dB(A), the structure has amplified the sound level by the simple difference between these two: 8 dB.

The second equation of interest relates the total level to its direct and reflected components:

$$L_{Total} = L_{Direct} \oplus L_{Reflected} \quad (2)$$

The circle around the plus sign signifies decibel addition. For example, if the direct component is 67 dB(A) and the reflected component is 74 dB(A), then the total level at the receptor will be the decibel sum of these two: 75 dB(A). Equation 2 can be rewritten as

$$L_{Reflected} = L_{Total} \ominus L_{Direct} \quad (3)$$

where the circle now signifies decibel subtraction. The example numbers are the same as those previously given:

$$74 \text{ dB(A)} = 75 \text{ dB(A)} - 67 \text{ dB(A)}.$$

Equation 1 is used to derive the amplification from the measured L_{Total} and the computed L_{Direct} . Equation 3 is used to derive the reflected component from these same two quantities.

In energy-like notation (to allow normal arithmetic rather than decibel arithmetic), Equation 3 converts to

$$10^{L_R/10} = 10^{L_T/10} - 10^{L_D/10} \quad (4)$$

Then Equation 4 is normalized by the emission level (L_{EL}) of the vehicle, the maximum passby level 50 ft to the side. Normalization of the first term on the right proceeds in two steps: first to L_{REF} at the reference microphone, and second to L_{EL} :

$$10^{(L_R - L_{EL})/10} = 10^{(L_T - L_{REF})/10} \times 10^{(L_{REF} - L_{EL})/10} - 10^{(L_D - L_{EL})/10} \quad (5)$$

$$10^{(L_R - L_{EL})} = (\text{Term 1}) (\text{Term 2}) - (\text{Term 3}) \quad (6)$$

Equation 6 identifies each of the terms of Equation 5 for easier discussion in the following sections, where each of these terms is discussed in detail.

Basic Data: Term 1 of Equations 5 and 6

Term 1 of Equations 5 and 6 comprises the basic data. This term is measured for each individual truck passby: L_{Total} at the receptor and L_{REF} simultaneously at the reference microphone. Precision is maintained in these simultaneous measurements by calibrating the ballistics of the two sound level meters.

A total of 219 heavy trucks (three or more axles) were measured. These data span a combination of 40 receptor and travel lane combinations, comprised of 10 receptor positions matched with 4 lower-roadway travel lanes.

Next, these data are separated by lane and receptor pairs into 40 subtables, each for a common lane and receptor pair. A standard error of 0.4 dB is typical of all 40 subtables.

In summary, there are 40 term 1's, each corresponding to one of the lane and receptor pairs. Each term 1 is the mean value of one of these 40 sub-tables divided first by 10, and then exponentiated on 10, as indicated in Equation 5. These 40 terms comprise truck noise levels normalized to the overhead reference microphone. Sufficient trucks are measured for each lane and receptor pair so that the mean is known within ± 1 dB.

Surrogate Term: Term 2 of Equations 5 and 6

Term 2 of Equations 5 and 6 converts the reference measurements to proper emission levels by independent experiment. The experiment is not in Austin, where the overhead roadways provide reflections, but instead at a similar cross-sectional site in San Antonio, where no overhead roadways exist. The reference microphone was supported on a cross-street bridge, as were the reference microphones in Austin. The level to the side was measured at one side position.

Figure 5 shows the cross-sectional geometry. The reference microphone is 35 ft above the travel lanes of the lower roadway and directly above the centerline of the slow travel lane. Because of this all sources extend to the left of this reference microphone position. The distance to the left is designated X. X ranges from zero for the slow travel lane, out to larger values for subsequent travel lanes, and ends at the slow travel lane in the opposite direction.

The side microphone is 5 ft above the pavement and 25 ft from the centerline of the nearest travel lane. Distance to the side microphone varies for each of the travel lanes, and all sideline levels are later converted to 50 ft. A regression equation is desired for the difference between the side and the overhead level as a function of which lane the vehicle is in.

Term 2 is not actually a difference in sound levels but instead is a ratio of energies associated with these sound levels. It is desirable to regress this ratio of energies directly, rather than to regress the differences in the exponent of 10 in these terms.

In addition, term 2 has one more complicating factor to it, as shown in Equation 7:

$$\begin{aligned} \text{Term 2} &= \left(10^{L_{REF}/10}/10^{L_S/10}\right) \left(10^{L_S/10}/10^{L_{EL}/10}\right) \\ &= \left(10^{L_{REF}/10}/10^{L_S/10}\right) [50/(25 + X)]^2 \end{aligned} \quad (7)$$

Term 2 does not just consist of the first factor in Equation 7, which relates the overhead reference microphone to the side level measured in this experiment. The second factor must also be included. This second factor is a distance conversion factor that converts the side microphone measurement to 50 ft (the standard distance for emission levels). This

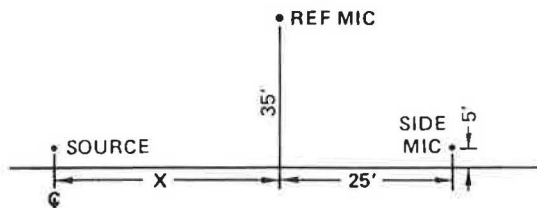


FIGURE 5 Independent experiment geometry to convert reference level to emission level.

entire term 2 is regressed, including the squared ratio term, so that the regression result is the full term 2. The result is

$$\text{Term 2} = 2.133 - 0.05933X + 0.0005371X^2 \quad (8)$$

This is the conversion to emission level from L_{REF} , the surrogate for emission level. It is an average term, averaged over the 69 trucks that passed by in San Antonio.

Computed Direct Level: Term 3 in Equations 5 and 6

Term 3 of Equations 5 and 6 is the computed sound level at the receptor, which ignores reflections from above. This computation proceeds in two steps:

$$\begin{aligned} \text{Term 3} &= \left[10^{(L_D/10) \text{ no barrier}}/10^{L_{EL}/10}\right] 10^{-A/10} \\ &= (50/D)^2 10^{-A/10} \end{aligned} \quad (9)$$

In this equation the first term is the distance correction term from the 50-ft distance of the emission level to the proper distance. The second term corrects for the barrier attenuation, which is a function of geometry.

The barrier-attenuation equations that underlay the FHWA barrier calculations were used. However, also used were the equations for a point source, rather than for a line source, because the peak passby level is the result of a single truck near its closest point of approach.

Note that Equation 9 does not contain vehicle emission level, which has been normalized out of the computation. In essence, this computation is a function only of the propagation between source and receptor.

RESULTING AUSTIN AMPLIFICATIONS

Figures 6 and 7 show the resulting amplifications in Austin. These amplifications follow from the measurements and from Equation 1. The resulting amplifications differ significantly between Austin Site 1 and Site 2. At Site 1 the noise increases are all large and do not drop off with distance from the roadway. At Site 2 the noise increases are smaller and drop off significantly as the receptor moves farther from the roadway.

To explain this site difference, ray-tracing techniques are used to search for a basic difference

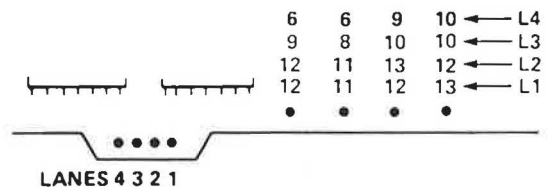


FIGURE 6 Resulting Austin amplifications, Site 1.

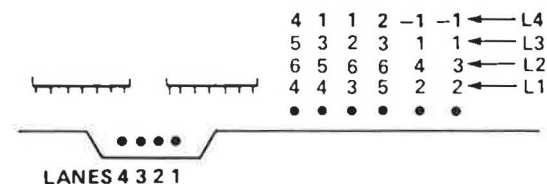


FIGURE 7 Resulting Austin amplifications, Site 2.

between Site 1 and Site 2. Figure 8 shows this basic difference. For Site 1, this figure shows that this site produces a unique triple bounce of truck noise, aimed directly at the receptors. This triple bounce occurs not only from the lane shown, but for all other lanes. It also occurs in several other manners. For example, from the lane shown, it bounces first off the roadway pavement, then to the opposite retaining wall, then to the overhead structure, then back down to the retaining wall, and then to the receptor. In effect, this is a quadruple bounce.

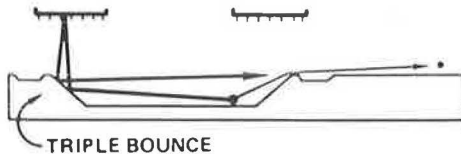


FIGURE 8 Site 1 anomaly.

This triple bounce for Site 1 results in additional paths by which sound can reach the receptors. These paths are quite similar to the direct path (shown lightly in the figure), except for two differences. First, they are longer, and second, they contain reflections.

These reflections are essentially specular because they are from the retaining wall and from the overhead structure, reflected perpendicularly. Because they are essentially specular, they result in a geometry that can be calculated, just as the direct geometry was calculated. This calculation was undertaken for each of the image sources that each receptor would see (i.e., bounced off the opposite retaining wall).

For each possible path, the expected level at the receptor was computed and subtracted from the total. In effect this means that the total sound level had many terms subtracted from it, not only the direct term, which goes directly over the retaining wall toward the microphone, but also each of these image terms. Even after this subtraction, however, Site 1 amplification is significantly more than that at Site 2.

What appears to be happening is the following: Sound generated by traffic and proceeding toward one of the retaining walls is bounced up to the overhead structure and back down to the retaining wall. This aims a significant amount of sound over to the opposite retaining wall, which then bounces it up to the opposite overhead roadway and back down again. In this manner sound is trapped between the two retaining walls, as if they were vertical. In reality they are not vertical, but the nearly 45-degree slopes of the retaining walls, combined with the horizontal overhead structure, in effect produces a vertical retaining wall. This results in a large amount of reverberant energy trapped in this depressed section. Each time the sound bounces off the overhead structure, some of it is scattered sideways by the structure to the receptor. After many bounces, significantly more sound is scattered sideways than would otherwise be there. This additional scattering makes Site 1 very different from Site 2.

Because of this triple-bounce anomaly at Site 1, which will not occur in San Antonio, the amplification results of Site 1 are not considered to be as relevant as those of Site 2. Both sets of results are retained in the analysis, nevertheless.

DIAGNOSIS OF REFLECTED SOUND

Combination of terms 1, 2, and 3 in Equation 5 yields the reflected portion of the sound at each receptor. This reflected portion is determined separately for each of the 40 lane and receptor pairs.

For many of these pairs there is no path by which sound can reflect off the upper roadway directly to the receptor with the angle of reflection equal to the angle of incidence. By pure ray-tracing reasoning, therefore, the sound for these pairs should not be amplified by the overhead structure.

Such pairs without direct specular reflections are as follows: for Site 1, for receptor 2: lanes 1 and 2; for receptor 3: lanes 1-3; and for receptor 4: lanes 1-4; and for Site 2, for receptor 3: lane 1; and for receptors 4-6: all lanes. The receptor numbers increase with distance from the roadway.

Nevertheless, for these lane and receptor pairs, amplification due to the upper roadway did occur. This portion of the amplification must be due to scattering from the upper roadway surface.

Figure 9 shows the reasoning behind the next steps of the analysis. For those lane and receptor pairs that have no chance of specular reflections, a regression analysis was undertaken to determine scattering as a function of the angles of interest. This scattering was subtracted from the other data to determine the residual component that remained. This residual was essentially zero, and therefore the other data were essentially all scattered as well.

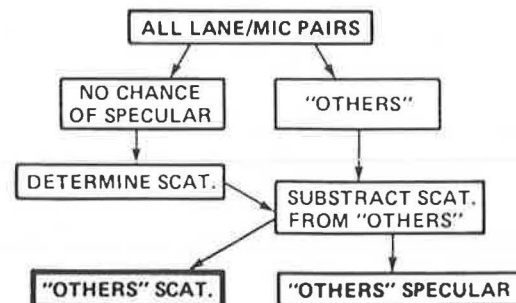


FIGURE 9 Overview of Austin diagnosis of reflected sound.

The scattering geometry is shown in Figure 10. For each lane and receptor pair, a line was drawn directly from the source up to the center of the reflecting surface and then down to the receptor. The two angles shown are the angle of incidence and the angle of scatter. This path has length D , which in general differs from 50 ft, the reference distance. Therefore, the total reflected component, normalized to the reference distance, is

$$10^{(L_R - L_{EL})/10} = (50/D)^2 F(\alpha_{inc}, \alpha_{scat}) \quad (10)$$

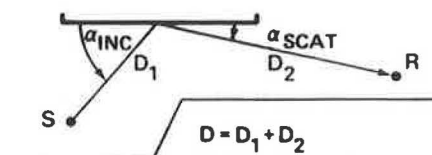


FIGURE 10 Scattering geometry.

In this equation F is the fraction of incident energy that is reflected toward the microphone. This fraction is a function of the two angles of concern, and it is this fraction that is sought.

Because the expression on the left has been previously measured for each of these lane and receptor pairs, and because the distance D is known, this equation can be used to solve for F . This was done for each of the lane and receptor pairs previously given. The average values of F are 0.62, 0.63, and 0.50 for Site 1 and 0.21, 0.34, 0.08, and 0.07 for Site 2.

As is apparent, Site 1 still does not match with Site 2; the scattered energy is far greater. For this reason, an attempt was made to interpret Site 1 data by a higher source height than for Site 2. Justification for this is as follows.

At Site 1 the trucks were coming out from underneath the cross-street overpass and accelerating up a grade of greater than 5 percent. Such acceleration results in two things. First, the emission levels of the trucks are increased. This is accounted for automatically by the reference microphone measurement directly above the truck. Second, most of the energy of an accelerating truck comes from the top of the stack of the truck, rather than from its tires, because the throttle is increased during acceleration. Thus the source height of these trucks is likely to be higher than it is for Site 2, where such upgrade acceleration did not occur.

For this reason all calculations were redone with a source height of 12 ft. The resulting Site 1 values of F were reduced by this increase in source height, but were still much larger than at Site 2.

A quadratic nonlinear fit was attempted on (a) all the data, including Site 1, and (b) on Site 2 data only. The statistics are as follows: On all data, $R^2 = 0.45$, and on the Site 2 data only, $R^2 = 0.73$. These fits are considered satisfactory for use and were retained as the final results. For F at both sites and no direct deflection,

$$F = 0.1435a_{inc} - 0.00171a_{inc}^2 + 0.02422a_{scat} - 2.731 \quad (11)$$

and for F_2 with no direct reflection,

$$F_2 = 0.1469a_{inc} - 0.001697a_{inc}^2 + 0.03225a_{scat} - 3.0709 \quad (12)$$

Equation 11 is later used for Site 1 data, and Equation 12 is used for Site 2 data.

As noted previously, many lane and receptor pairs were left out of this regression analysis. These were left out because, for these pairs, strong single specular reflection is possible.

The next obvious question is how well the regression fit explains the lane and receptor pairs that were not used in its development. In other words, each of the pairs that has a direct specular reflection also has an angle of incidence and an angle of scatter. Therefore, they would probably also have a portion of the excess energy contributed by scattering. In essence, this scattered portion is found by using the regression equations. Then, after subtracting it from the total sound for those pairs, the remainder is the portion that would arrive by way of direct specular reflection.

Results indicate that, except for the first two lane and receptors pairs, the specular reflections have no influence on the measured noise levels. All of the energy arrives by way of scattering. Even for the first two pairs, scattering controls the amplification at the microphone position.

It is concluded from this analysis that all the amplification to the side in Austin is caused by

scattering, and essentially none is caused by specular reflection.

A FINAL CHECK: SPECULAR PREDICTIONS FOR AUSTIN

The specular amplification for the Austin geometry was next predicted for comparison with the measured scattered amplification. In this manner the difference between specular and scattered conditions could be directly determined. The results of the specular calculations are described herein.

The basic equation is

$$L_T = (L_D - A) + (\sum L_R) \quad (13)$$

dB sum, also

This equation states that the total measured noise level is the sum of the direct level (minus the barrier attenuation) and all reflected levels received by reflected paths. All these sums are decibel summations.

The results of this analysis appear as dotted lines in Figures 11 and 12 as a function of distance from the edge of the structure. For comparison, the solid line shows the measured amplification in Austin. The measured amplification significantly exceeds the specular predictions, as is obvious from the figures.

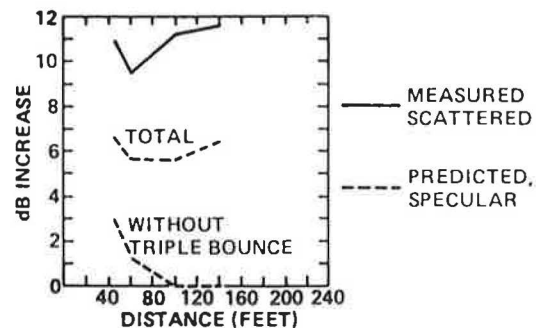


FIGURE 11 Austin comparisons of measured amplification and specular predictions, Site 1.

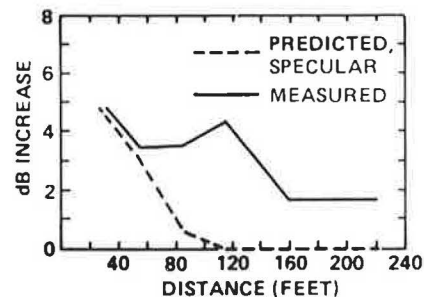


FIGURE 12 Austin comparisons of measured amplification and specular predictions, Site 2.

Figure 11 shows a breakdown of the specular amplification into that produced by the triple bounce and that produced by the remainder of the reflections. As is obvious from Figure 11, most of the amplification is from the triple bounce and little is from the remaining reflections. This check on specular reflections confirms the diagnosis that scattering predominates over specular reflection from the underside of the Austin structure.

VERIFICATION

Overview

The measurements previously cited are best called diagnostic measurements. They involve individual truck passbys, where the lane of travel is known for each passing truck. During the closest point of approach for each such truck, noise from that truck completely dominates the total sound level at the receptor. The measurement then allows diagnosis of the path(s) that this noise has traveled from truck to receptor.

Such diagnostic measurements could not have been made by using the full noise climate at the receptor. This full noise derives from many different vehicles, each with its own emission level, and from vehicles traveling on many different lanes. The propagation situation is simply too complicated for diagnosis.

Another way of looking at the diagnosis is that the diagnostic measurements were of short duration, essentially just a second or less, when an individual truck was registering its maximum noise level at the receptor. During this short duration one noise source dominated. The situation is relatively simple. On the other hand, longer measurements capture many vehicles and much more complexity. These longer measurements do not allow diagnosis.

It was thought desirable, notwithstanding these difficulties, to measure noise during some longer periods to determine if the results of the diagnosis would adequately predict the longer-term noise levels; specifically, the energy-average noise level L_{eq} . For this purpose a series of verification measurements was made.

Verification measurements were made at Site 2, as well as at two additional sites along the elevated sections of I-35 in Austin. These two additional sites are both sites where the lower roadway is at grade. They differ from each other in that the elevated roadway is significantly higher at one than at the other.

Method

At each of these three verification sites a series of 10-min L_{eq} 's was obtained. Simultaneously, the traffic was classified and speeds were measured. In addition, overhead noise levels were measured for each passing heavy truck for later conversion to emission levels. Then, by using these measured data at the site, the L_{eq} 's were predicted for each 10-min period for matching with the measured 10-min L_{eq} 's.

The L_{eq} noise predictions were made in accordance with the current FHWA method (1), as embodied in FHWA's (Texas Instruments) programmable-calculator program. Instead of using the national average emission levels for heavy trucks on the lower roadway, emission levels specific to the measurement period were obtained from the overhead reference levels. These emission levels, specific to I-35 in Austin and specific to the actual 10 min of measurement, were used only for heavy trucks on the lower roadway. The national average emission levels were used in all other cases.

Full traffic classifications were made for the lower roadway, separately by lane, and also for the near frontage road. These classifications were made simultaneously with the noise measurements. Classification on the upper roadway was done only by direction of travel, either before the period of measurement or after it, generally within 2 hr of the

measurement. Although this time displacement for the upper roadway results in only an approximate classification during measurement, traffic from this roadway is shielded from the receptors by the edge of structure. It does not dominate the noise.

Speeds were measured on the lower roadway and the near frontage road by timing a sample of heavy trucks between two fixed points. The average of these sampled speeds was used for computation.

Volumes and speeds on the far frontage road were taken to be identical to those measured on the near frontage road. All barrier calculations were done separately by lane and separately by the three vehicle types: automobiles (all four-tire vehicles), medium trucks (all six-tire vehicles), and heavy trucks (all vehicles with more than six tires). For these barrier calculations, all traffic on the two elevated structures was positioned in the lane nearest the receptor.

The noise calculations were kept separate by lane and by vehicle type for each 10-min period. Before combining them into the total 10-min noise level, the heavy-truck contributions on the lower roadway were adjusted to account for the level difference between the national average emission (ignoring grade) built into the FHWA method and the measured emission levels during the measurement period.

First, the overhead reference levels were converted to sideline emission levels at 50 ft by using the following equation:

$$L_{REF} - L_{EL} = 10 \log(2.133 - 0.05933X + 0.0005371X^2) \quad (14)$$

where X is the horizontal distance between the reference microphone and the centerline of the lane of travel, as before. Then emission levels of all the heavy trucks that passed during the 10-min period were energy-averaged to obtain the average emission level for that measurement period.

A total of 329 heavy trucks were measured over the total of 21, 10-min verification periods, for an average of 16 trucks per period. Note that this number of trucks is not a small sample; it is all the heavy trucks that passed during the measurement periods and comprises the full population of trucks that should be used for emission level adjustment. The heavy-truck emission level adjustments, relative to the national average emission levels, ranged between -7 and +2 dB, averaging -2.1 dB.

Another complication enters here. The overhead reference levels for these trucks were measured at the closest cross-street bridge that passed over the lower roadway. For verification of Site 1 data, which was identical to a diagnostic site, this closest bridge was immediately adjacent, where the lower roadway was fully depressed. For the other two verification sites, however, the nearest cross-street bridge was a distance from the measurement site.

Of most importance here is that the overhead measurement occurred where the trucks were in a depressed section, whereas for the verification the sideline measurement occurred where they were at grade. It is possible that truck drivers use different amounts of throttle for these two different positions along their travel, and it is possible that this throttle change introduces a bias in the computation method.

To check for such a bias and to compensate for it if found, the sideline noise of 51 heavy trucks was measured along I-35 in San Antonio at a location where the cross section alternated between depressed and at grade (similar to Austin). Distinction was made between trucks passing in the two different

directions. For these trucks in San Antonio, the differences in emission levels were

Direction 1: $L_{\text{depressed}} - L_{\text{up-grade}} = 0.3$ dB,
 Direction 2: $L_{\text{depressed}} - L_{\text{up-grade}} = -0.8$ dB, and
 Full average: $L_{\text{depressed}} - L_{\text{up-grade}} = 0.2$ dB.

Within experimental error, this small level difference is not significantly different from zero. Therefore, no adjustment was made to account for the fact that the overhead measurements were not made immediately adjacent to the sideline measurements for verification Sites 2 and 3.

After emission level adjustments were made for all lower-roadway heavy trucks, the contributions from all vehicles on the lower roadway and frontage roads were increased by reflection from the underside of the structure. In total,

$$10^{L_T/10} = 10^{L_R/10} + 10^{L_D/10} \times 10^{-A/10} \quad (15)$$

where A equals the barrier attenuation for this particular lane, vehicle, and receptor combination. Note that L_D is the direct contribution without barrier attenuation. Next,

$$10^{L_R/10} = 10^{L_D/10} (D_D/D_R)^1 F \quad (16)$$

where the distance ratio is taken to the power of unity because the L diverges as a line source. The fraction F is the fraction of energy lost on reflection from the upper surface:

$$F = 0.1469a_{\text{inc}} - 0.001697a_{\text{inc}}^2 + 0.03225a_{\text{scat}} - 3.0709 \quad (17)$$

from the scattering measurements at diagnostic Site 2. Next, the amplification due to reflection is

$$\text{Amp} = L_T - (L_D - A) \quad (18)$$

In total,

$$\text{Amp} = 10 \log \{ [0.1469a_{\text{inc}} - 0.001697a_{\text{inc}}^2 + 0.03225a_{\text{scat}} - 3.0709] (D_D/D_R) + 10^{-A/10} \} + A \quad (19)$$

This equation was used to compute the overhead amplification separately for each lane, vehicle, and receptor combination for a total of 55 amplification computations.

Finally, once these two adjustments were made (emission level and amplification), the contributions from all lanes were summed to the total 10-min L_{eq} .

Results

On average, the predictions agree with measurements within 1 dB, which is better than could generally be hoped. For closeby receptor positions, predictions fall below measurements by 3 to 5 dB; in other words, the predictions are too low. There exists the possibility that the predicted amplification from the structure is too low. This is most likely not the case, however, because the amplification was measured precisely during the diagnostic measurements, which are far more controlled than are these verification measurements. In addition, the verification predictions have many possible sources of bias not connected with the upper structure. Perhaps

the FHWA method under-predicts the noise from the frontage road traffic, which is generally stop-and-go traffic. According to the computations, this frontage road traffic was a significant contributor to the total noise level, especially for the closeby receptor positions, basically because it is so close.

For receptor positions that are farther out, predictions are greater than measurement by 1 to 7 dB; that is, predictions are too high. This is most likely due to shielding, in plan, which intervenes between the receptors and the traffic lanes, both to the right and to the left of the closest point of approach. This shielding was not taken into account in the computations. In addition, the over-prediction could result partly from the assumption of hard ground between source and receptors ($\alpha = 0$ in the FHWA method). This hard-ground assumption is more nearly true, on average, than it would be for the soft-ground assumption because of the street or driveway down which the receptor line was placed, but a significant amount of the intervening ground was grass.

In summary, the verification measurements do not dispute the results obtained from the diagnostic measurements. For this reason, they lead to no changes in the conclusions of the study. The verification measurements are shown in Figure 13.

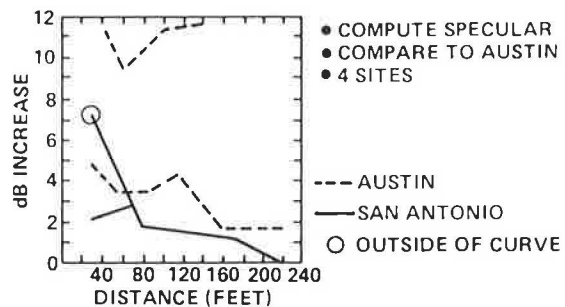


FIGURE 13 Summary of Austin verification measurements.

SAN ANTONIO COMPUTATIONS

Four typical sites were chosen for analysis in San Antonio: depressed, vertical retaining walls; depressed, grassed slopes; flat; and 10-lane elevated. At these cross sections the noise from all vehicles on the lower roadway was computed, assuming specular reflection from above.

These calculations were made with the official FHWA highway noise traffic prediction model embodied in its programmable-calculator form. Therefore, they all assume infinite roadway and infinitely long barriers. Source height assumptions were zero height for automobiles, 2.8 ft for medium trucks, and 8 ft for heavy trucks. These source heights are important to barrier calculations.

Calculations were made for every travel lane and for the three vehicle types at every receptor location. Receptor locations were chosen to be at the closest building lines and 5 ft above the local terrain. At the fourth site an additional receptor location was placed 15 ft above the local terrain to account for noise entering the second story at this site.

In Figure 14 the results are condensed as a function of distance from the edge of the structure, where they are compared with the Austin results. At 30 ft the two sides of the roadway differ appreciably, as shown in the figure.

In conclusion, the noise in San Antonio increases

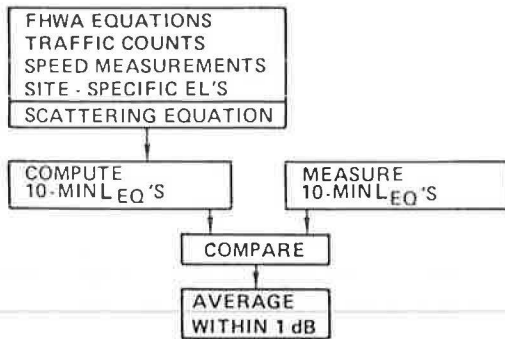


FIGURE 14 Predicted San Antonio amplification compared with Austin measurements.

to the side due to overhead reflections, and it should be less than that measured in Austin, except when both of the following occur: (a) the receptor is within 50 to 60 ft of the edge of the elevated structure, and (b) the upper roadway curves away from the receptor. When the upper roadway curves away from the receptor, its tilted undersurface

tends to aim energy toward the receptor, thereby increasing the noise. The San Antonio values of 2 and 7 dB on the graph occurred at such a roadway curve, on opposite sides of the roadway.

The particular 10-lane elevated section chosen for study in San Antonio is unique. It occurs where the frontage road runs underneath the upper roadway. For most of the 10-lane elevated section there is no roadway underneath to be amplified. For this calculated cross section, where the frontage road is underneath, the upper roadway increases frontage roadway noise to the side by approximately 3 to 4 dB.

REFERENCE

1. Highway Traffic Noise Prediction Model. Report FHWA-RD-77-108. FHWA, U.S. Department of Transportation, Dec. 1978.

Publication of this paper sponsored by Committee on Transportation-Related Noise and Vibration.

Evaluation of T-Profile Highway Noise Barriers

J. J. HAJEK and C. T. BLANEY

ABSTRACT

An acoustical performance evaluation of unique 5-m-high sound-absorbing parallel highway noise barriers, with a horizontal cap to form a T-profile, is presented. The evaluation was done by using (a) direct field measurements, (b) analytical procedures based on the STAMINA 2.0 computer program and the application of geometrical acoustics, and (c) acoustical scale modeling. Noise measurements in the residential area behind the barriers indicated that the addition of a 1-m-wide horizontal cap on top of the barrier had increased its insertion loss by about 1 dB(A). Similar results were obtained by acoustical scale modeling, which also indicated that it is usually acoustically more effective to increase the barrier height rather than to build a T-top.

The objective of this paper is to present the results of an acoustical evaluation of unique parallel highway noise barriers constructed in 1983. The barriers have sound-absorptive layers on both the highway and the residential sides. A 1-m-wide sound-

absorptive cap is mounted horizontally on top to create a T-profile.

The evaluation has been conducted by using direct field measurements, analytical calculations, and acoustical scale modeling. The latter two methods were used to establish their accuracy in relation to the field measurements and to evaluate various design parameters, such as the T-top shape and absorptive treatment of barrier walls, which could not be evaluated effectively in the field.

The barriers are located along both sides of the Queen Elizabeth Way (QEW), east of Cawthra Road in Mississauga, Ontario. At this location the QEW has six traffic lanes, three in each direction, and the barriers are about 36 m apart. On both sides of the QEW there are two-lane service roads. The terrain is flat, gently sloping toward the south (Lake Ontario). Figure 1 shows the general barrier setting, together with the location of T-top and conventional barriers, and the measurement locations used for evaluation.

The photographs in Figures 2 and 3 have been included to illustrate the appearance and aesthetics of T-top barriers. Although opinions in these matters can certainly differ, the addition of the horizontal cap does not appear to degrade the appearance of a conventional type barrier.

Construction of noise barriers at this site had been anticipated during highway construction in 1977. Thus 0.8- to 1.2-m-high New Jersey (NJ) type